ELSEVIER

Journal of Crystal Growth 156 (1995) 39–44

JOURNAL OF CRYSTAL GROWTH

Growth of GaInAsSb alloys by metalorganic chemical vapor deposition

Shuwei Li *, Yixin Jin, Tianming Zhou, Baolin Zhang, Yongqiang Ning, Hong Jiang, Guang Yuan, Xinyi Zhang, Jinshan Yuan

Chang Chun Institute of Physics, Academia Sinica, 130021 Chang Chun, People's Republic of China

Received 20 May 1995; manuscript received in final form 13 June 1995

Abstract

GaInAsSb alloys were grown by atmospheric pressure metalorganic chemical vapour deposition (MOCVD) on n-GaSb (Te-doped) substrates, oriented 2°–3° off (100) towards ⟨110⟩. The surface morphology of Sb-related III–V compounds depends on the growth parameters, the lattice mismatch and the quality and orientation of the surface of the substrate. The defect growth process is observed by scanning electron microscopy (SEM) and scanning electron acoustic microscopy (SEAM). The Ga and Sb concentrations in the solid were characterized as a function of the input ratio of Sb to group V, the AsH_3 molar flow rate and growth temperature. On the other hand, the growth efficiency has been studied versus the AsH_3 molar flow and growth temperature. The crystalline quality of the GaInAsSb epilayer has been characterized by the single-crystal X-ray diffraction pattern and double-crystal X-ray rocking curve diffraction.

1. Introduction

III–V antimonide compounds have several important applications, including optical communication employing fluoride-based fibres [1], laser radar exploiting atmospheric transmission windows, remote sensing of atmospheric gases and molecular spectroscopy. These compounds are most suitable because of the possibility to choose the composition in the quaternary GaInAsSb alloy system with the direct band gap adjustable in the wavelength range from 1.7 to 4.3 μm. The compounds can be grown lattice-matched on GaSb, InAs and InP substrates, which may provide the basis for emitters and detectors over this entire frequency region. A GaInAsSb alloy grown by liquid phase epitaxy (LPE) was first reported in 1976 [2]. There is such a miscibility gap for the GaInAsSb alloy grown by equilibrium growth techniques such as LPE; so it is difficult to grow GaInAsSb alloys which have a miscibility gap using LPE. The metastable GaInAsSb alloys with compositions in the miscibility gap can be grown using non-equilibrium techniques, such as molecular beam epitaxy (MBE) [3] and metalorganic chemical vapor deposition (MOCVD) [4]. In 1988, Bougnot et al. reported that $Ga_xIn_{1-x}As_{1-y}Sb_y$ alloys for $x, y > 0.8$ had been grown by MOCVD and the spectral response of $Ga_{0.78}In_{0.22}As_{0.20}$

* Corresponding author.

SSDI 0022-0248(95)00274-X

$Sb_{0.80}$/GaSb p–n photodiodes showed a wavelength cut off at 2.4 μm at room temperature. In this paper the growth of GaInAsSb alloys by MOCVD is described. Using the method reported by Moon [5], we obtained an energy–composition relation of $Ga_xIn_{1-x}As_{1-y}Sb_yE_g$ $(x, y) = 0.359 + 0.48x - 0.78y - 0.398xy + 0.6x^2 - 0.596y^2 + 0.185x^2y + 0.054xy^2$.

2. Experimental procedure

The alloys of GaInAsSb were grown on GaSb substrates by MOCVD using a conventional atmospheric pressure horizontal reactor. The sources of Ga, In, Sb and As were trimethylgallium (TMGa), trimethylindium (TMIn), trimethylantimony (TMSb) and arsine (AsH_3) diluted to 10% in hydrogen, respectively. TMGa, TMIn and TMSb were carried out using Pd-diffused hydrogen into the reactor. The substrates were n-GaSb (Te-doped) oriented 2°–3° off (100) towards ⟨110⟩. GaSb was cleaned by degreasing in solvents and deionized water. It was then chemically polished by a solution of $HNO_3 : HCl : CH_3COOH = 0.2 : 2 : 20$ for 15 min, rinsed with deionized water and blown dry with nitrogen to put into the reactor. Some key growth parameters are listed in Table 1.

3. Scanning electron acoustic microscopy (SEAM) and morphology of surface and subsurface

Scanning eletron acoustic microscopy (SEAM) also referred to as thermal wave microscopy was developed in 1980 and has been used in the last years for the characterization of many materials [6]. SEAM as new experimental tool has been successively applied for polarization distribution, phase transition, subgrain boundaries and domain structure in polar materials and nondestructive observation of internal phenomena in many other materials and devices [7,8]. The mechanism of the electron acoustic signal generated by SEAM is different for different kind of materials. The present work is a preliminary study of the capabilities of SEAM in the characterization of the GaInAsSb alloy. SEAM was constructed using conventional scanning electron microscopy to which several newly designed parts, a flexible plug-in beam blanking system, an opto-electric coupler and a spring loaded and metal shielded PZT electron acoustic signal detector were attached.

Table 1
Growth parameters of the GaInAsSb alloys

Total H_2 flow rate (ℓ/min)	3.3–4.5
TMGa source temperature (°C)	−14
TMGa molar flow rate (μ mol/min)	2–10
TMIn source temperature (°C)	15
TMIn molar flow rate (μ mol/min)	2–5
TMSb source temperature (°C)	0
TMSb molar flow rate (μ mol/min)	9–18 AsH_3 molar
flow rate (μ mol/min)	1–3
(III/V) ratio	0.4–1.3
Growth temperature (°C)	570–640

The surface morphology of Sb-related III–V compounds grown by MOCVD depends on the growth parameters, the lattice mismatch and the quality and the orientation of the surface of the substrate. The epilayers of GaInAsSb with a mirror-like surface grown by MOCVD were obtained only in a narrow range of growth parameters. Pyramid-like hillocks with a rectangular basal plane are usually observed. The surface density of the pyramid-like hillocks depends upon the growth parameters and decreases with growth rate and lattice mismatch. Fig. 1 shows the scanning eletron microscopy (SEM) and SEAM images of the $Ga_{0.79}In_{0.21}As_{0.18}Sb_{0.82}$ alloy in situ. Comparison of SEM and SEAM images shows that the two techniques provide different information. Fig. 1a shows a SEM image of pyramidal hillocks parallel with the ⟨110⟩ axis on the surface of the sample, Figs. 1b and 1c show in situ SEAM images with defects at different crystal slab thicknesses below the surface. The electron beam characteristics had a chopping frequency between 30 and 500 kHz, a duty ratio of 50%, an acceleration voltage of 20–30 kV, and a maximum beam current of 4×10^{-6} A.

4. Growth results and discussion

For convenience to calculate the ratio of group-III to group-V elements and the ratio of Sb

to total group-V elements based on the input partial pressures, we will define the III/V ratio to be $(P_{TMGa}+P_{TMIn})/(P_{TMSb}+P_{AsH_3})$, Ga/III to be $P_{TMGa}/(P_{TMGa}+P_{TMIn})$ and Sb/V to be

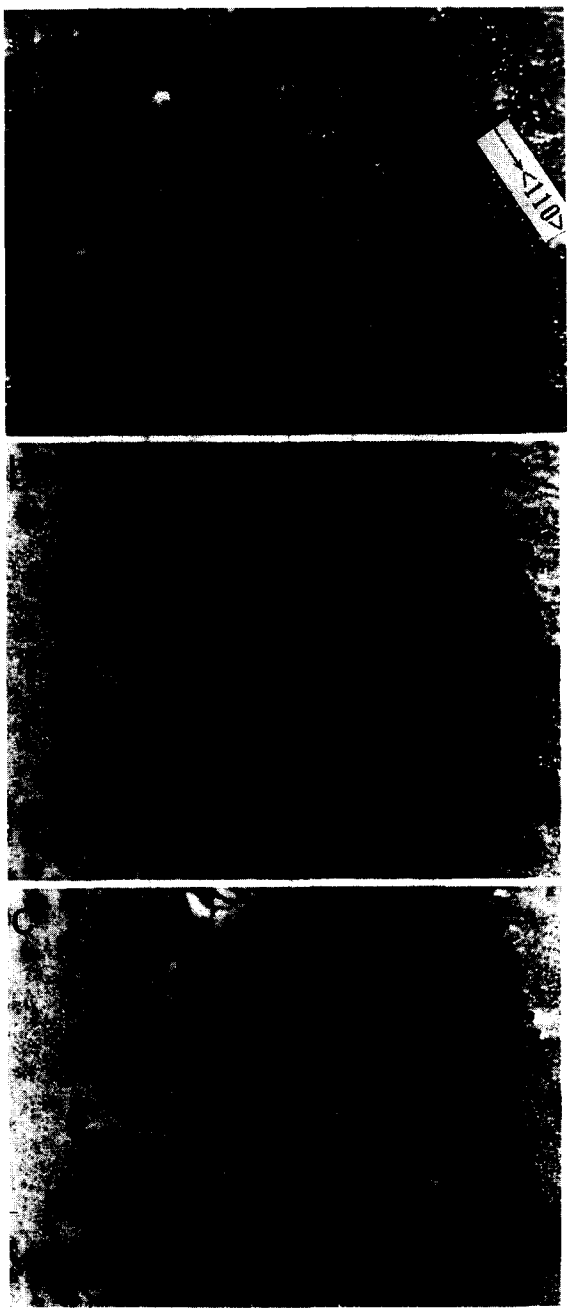

Fig. 1. (a) SEM image. (b) SEAM image $f = 456$ KHz, mag. = 200. (c) SEAM image $f = 341$ KHz, mag. = 200.

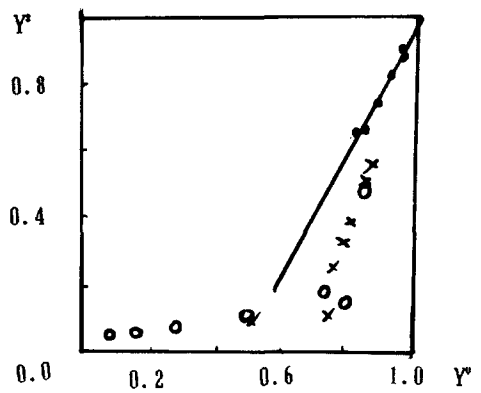

Fig. 2. The composition y of $Ga_xIn_{1-x}As_{1-y}Sb_y$ in the solid versus the composition y^v in the vapor phase $[y^v = P_{TMSb}/(P_{TMSb}+P_{AsH_3})]$.

$P_{TMSb}/(P_{TMSb}+P_{AsH_3})$. The Sb concentration in the solid is plotted versus the input ratio of Sb to group-V elements in Fig. 2 with constant values of III/V = 0.75 and a growth temperature of 600°C. In Fig. 2 data marked as (·) were obtained by us, data marked as (×) were obtained from S.M. Bedair et al. in GaAsSb [9], and data marked as (○) were obtained by T. Fukui et al. in InAsSb alloys [10]. In the GaSb-rich region, the Sb concentration is directly proportional to the input ratio of Sb to group-V with constant values of (III/V). On the other hand the Sb concentration is affected by the absolute molar flow rate of group-V elements.

The dependence of the Ga and Sb concentration in the solid on the AsH_3 flow rate for fixed values of (Ga/III) = 0.7, (Sb/V) = 0.93 and growth temperature 600°C is shown in Fig. 3. With the fixed values of (Ga/III) and (Sb/V), a slow decrease in Sb composition with increasing AsH_3 flow rate and a constant value of Ga composition with increasing AsH_3 flow rate are observed. In other words, the Sb concentration is decreased and the Ga concentration is fixed with the input total molar flow rate.

The dependence of the Ga and Sb concentration in the solid on the growth temperature for several fixed values of (III/V) = 0.75, (Ga/III) = 0.80 and (Sb/V) = 0.87 are shown in Fig. 4. The Ga concentration is plotted, first, for the fixed values of (III/V), (Ga/III) and (Sb/V), and the

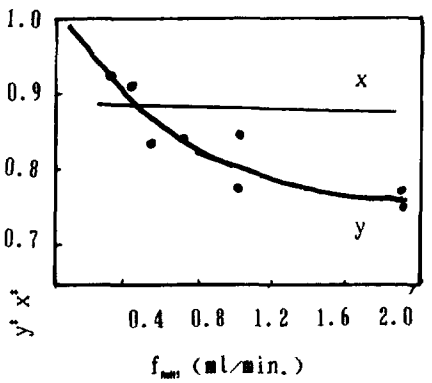

Fig. 3. The influence of the flow rate of AsH_3 on the composition of $Ga_xIn_{1-x}As_{1-y}Sb_y$ in the solid phase. $T_g = 600°C$, (Sb/V) = 0.93, (Ga/III) = 0.7.

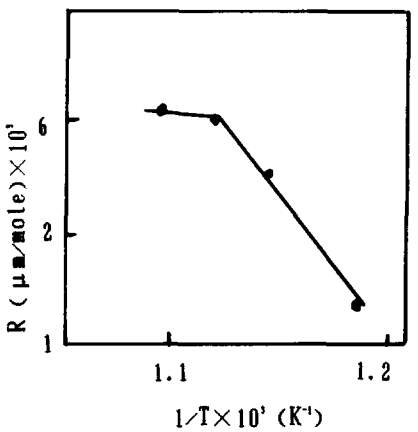

Fig. 5. The growth rate (R) of $Ga_xIn_{1-x}As_{1-y}Sb_y$ versus growth temperature (T_g). III/V = 0.74, Ga/III = 0.80, Sb/V = 0.87.

Ga concentration increases with increasing growth temperature; in addition, at growth temperatures higher than 620°C, the Ga concentration appears to reach a nearly constant value. The Sb concentration is plotted, for growth temperatures higher than 600°C and a slow decrease in Sb composition is observed; however, for growth temperatures below 600°C, the Sb composition is seen to decrease sharply with decreasing temperature. It is reasonable to assume that TMIn pyrolysis is complete for a temperature higher than 500°C [11], TMGa pyrolysis increases with increasing temperature below 620°C and is complete for temperatures higher than 620°C. So, the Ga concentration increases with increasing growth temperature and becomes constant for a growth temperature higher than 560°C. For growth temperatures higher than 600°C, AsH_3 pyrolysis increases with increasing growth temperature [12] and TMSb pyrolysis is complete; meanwhile, the Sb concentration decreases which increasing growth temperature. Below 600°C, TMSb pyrolysis decreases sharply with decreasing growth temperature; so, the Sb concentration decreases sharply.

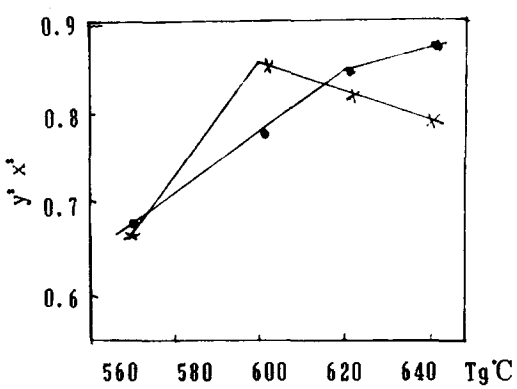

Fig. 4. The composition of $Ga_xIn_{1-x}As_{1-y}Sb_y$ in the solid phase versus the growth temperature. III/V = 0.75, Ga/III = 0.80, Sb/V = 0.87.

The growth efficiency, defined as the ratio of the growth rate to the group-III molar flow rate, is plotted versus growth temperature in Fig. 5. Two growth regimes are observed. When the growth temperature is higher than 620°C, the growth efficiency is found to be nearly constant. For temperatures lower than 600°C, the growth efficiency is dependent on the temperature. The temperature dependence of the GaInAsSb growth efficiency indicates that surface kinetics control the growth rate. It seems likely that TMGa pyrolysis is complete for temperatures below 620°C. The thermodynamic equilibrium model of Stringfellow [13] predicts that the group-III partial pressure at the interface is very small when the input V/III ratio is greater than unity. Thus, incomplete pyrolysis of TMGa will reduce the growth rate and affect the group-III distribution coefficient, but will have little or no effect on the group-V distribution coefficient. The growth efficiency of GaInAsSb alloys is plotted versus the

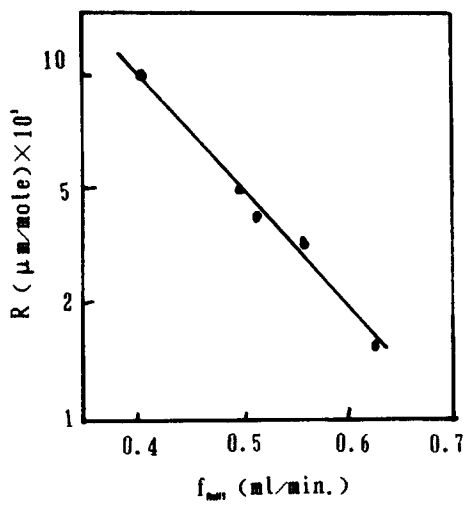

Fig. 6. The growth rate (R) of $Ga_xIn_{1-x}As_{1-y}Sb_y$ versus flow rate of AsH_3 (f_{AsH_3}). $T_9 = 600°C$, Sb/V = 0.87.

flow rate of AsH_3 in Fig. 6 with constant values of (Sb/V) = 0.87 and growth temperature 600°C. For a temperature of 620°C, the growth efficiency is inversely proportional to that of the AsH_3 flow rate; in other words, the binding rate of the group-III elements decreases with increasing AsH_3 flow rate.

The single-crystal X-ray diffraction pattern of the $Ga_{0.19}In_{0.21}As_{0.14}Sb_{0.86}$ epilayer on the GaSb substrate shown in Fig. 7a illustrates good crystallinity. Fig. 7b shows the double-crystal X-ray rocking curve of the (400) diffraction of GaInAsSb having a fwhm of 6 arc min which shows that a high crystalline quality was obtained. p^+-GaInAsSb/p-GaInAsSb/n-GaSb infrared detectors are obtained with GaInAsSb alloys. The spectral responses of p^+-GaInAsSb/ p-GaInAsSb/n-GaSb detectors showed a wavelength cut off at 2.4 μm, the quantum efficiency at 2.25 μm is about 40% and detectivity $D^* = 2 \times 10^9$ cm $Hz^{0.5}/W$ at room temperature.

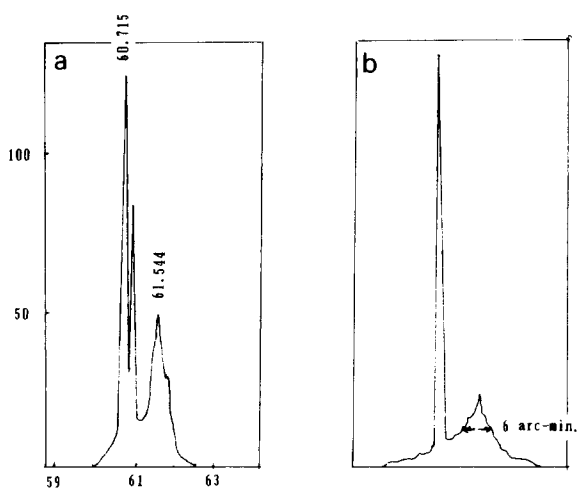

Fig. 7. (a) The X-ray diffraction pattern. (b) The double-crystal X-ray rocking curve.

5. Conclusion

GaInAsSb alloys have been successfully prepared by AP-MOCVD using TMGa, TMIn, TMSb and AsH_3 as source materials. The results of X-ray single-crystal diffraction and double-crystal rocking curve diffraction indicated that GaInAsSb alloys are high-quality solid solutions. On the other hand, a defect growth process has been obtained. The experimental results shown in this paper indicate that SEAM reveals internal information of the specimen.

Acknowledgements

The authous wish to thank Jiang Fuming, Yin Qingrui and Zhang Bingyang of Shang Hai Institute of Ceramics, Academia Sinica for the SEAM images. This work was supported by the National Advanced Material Committee of China under grant 863-715-01-02-02.

References

[1] S. Shibata, M. Horiguchi, K. Jinguji, S. Mitachi, T. Kanamori and T. Manabe, Electron. Lett. 17 (1981) 775.
[2] R. Sankaran and G. Antapas, J. Crystal Growth. 36 (1976) 198.
[3] W.T. Tsang, T.H. Chin, D.W. Kisker and J.A. Pitenberger, Appl. Phys. Lett. 48 (1985) 283.
[4] M.J. Cherng and G.B. Stringfellow, Appl. Phys. Lett. 48 (1985) 419.
[5] R.L. Moon, G.A. Antypas and L.W. James, J. Electron Mater. 3 (1974) 635.

[6] P. Fernadez, J. Llopis and J. Piqueras, Mater. Chem. Phys. 24 (1989) 215.
[7] M. Urchulutegui, J. Piqueras and J. Llopis, J. Appl. Phys. 65 (1989) 18.
[8] M. Urchulutegui and J. Piqueras J. Appl. Phys. 69 (1991) 15.
[9] S.M. Bedair, M.L. Timmons and P.K. Chiang, J. Electron Mater. 12 (1987) 959.
[10] T. Fukui and Y. Horikoshi, Jpn. J. Appl. Phys. 19 (1980) L53.
[11] C.A. Larsen and G.B. Stringfellow, J. Crystal Growth 75 (1986) 247.
[12] G.B. Stringfellow, J. Crystal Growth 68 (1984) 111.
[13] G.B. Stringfellow, J. Crystal Growth 62 (1983) 417.